

Supplementary materials

The LiNbO₃-type to perovskite-type transition and ferric-iron-rich silicate in the transition zone

Mingda Lv¹, Shengcai Zhu^{2*}, Jiachao Liu¹, Yi Hu^{3,4}, Feng Zhu^{5,6}, Xiaojing Lai^{3,4,7}, Dongzhou Zhang³, Bin Chen³, Przemyslaw Dera³, Jie Li⁵, and Susannah M. Dorfman^{1*}

¹ Department of Earth and Environmental Sciences, Michigan State University, East Lansing, MI, USA

² School of Materials, Sun Yat-Sen University, Guangzhou, China

³ Hawai'i Institute of Geophysics and Planetology, University of Hawai'i at Mānoa, Honolulu, HI, USA

⁴ Department of Geology and Geophysics, School of Ocean and Earth Science and Technology, University of Hawai'i at Mānoa, Honolulu, HI, USA

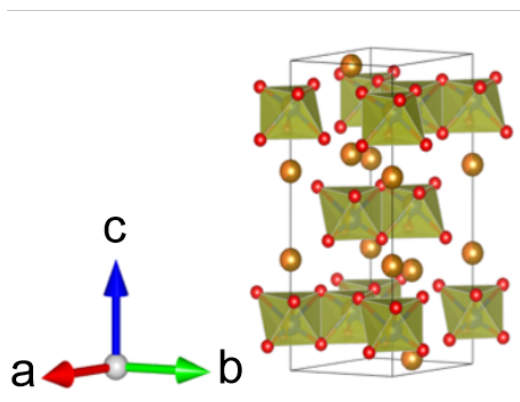
⁵ Department of Earth and Environmental Sciences, University of Michigan, Ann Arbor, MI, USA

⁶ State Key Laboratory of Geological Processes and Mineral Resources, School of Earth Sciences, China University of Geosciences, Wuhan, Hubei, China

⁷ Gemological Institute, China University of Geosciences, Wuhan, Hubei, China

* Corresponding authors: S.M. Dorfman (dorfman3@msu.edu) and S. Zhu (zhushc@mail.sysu.edu.cn)

(a) ilmenite-type structure



(b) LiNbO_3 -type structure

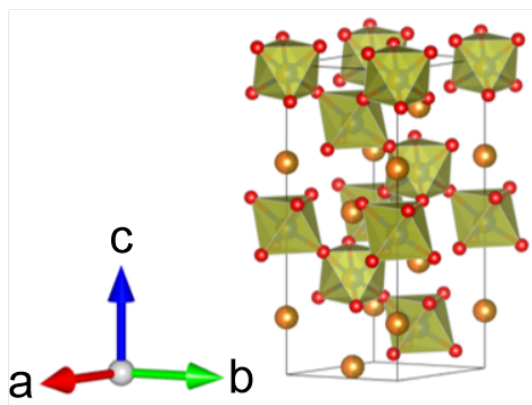


Figure S1. Crystal structure of MgSiO_3 with (a) $R\bar{3}$ ilmenite-type structure and (b) $R3c$ LiNbO_3 -type structure.

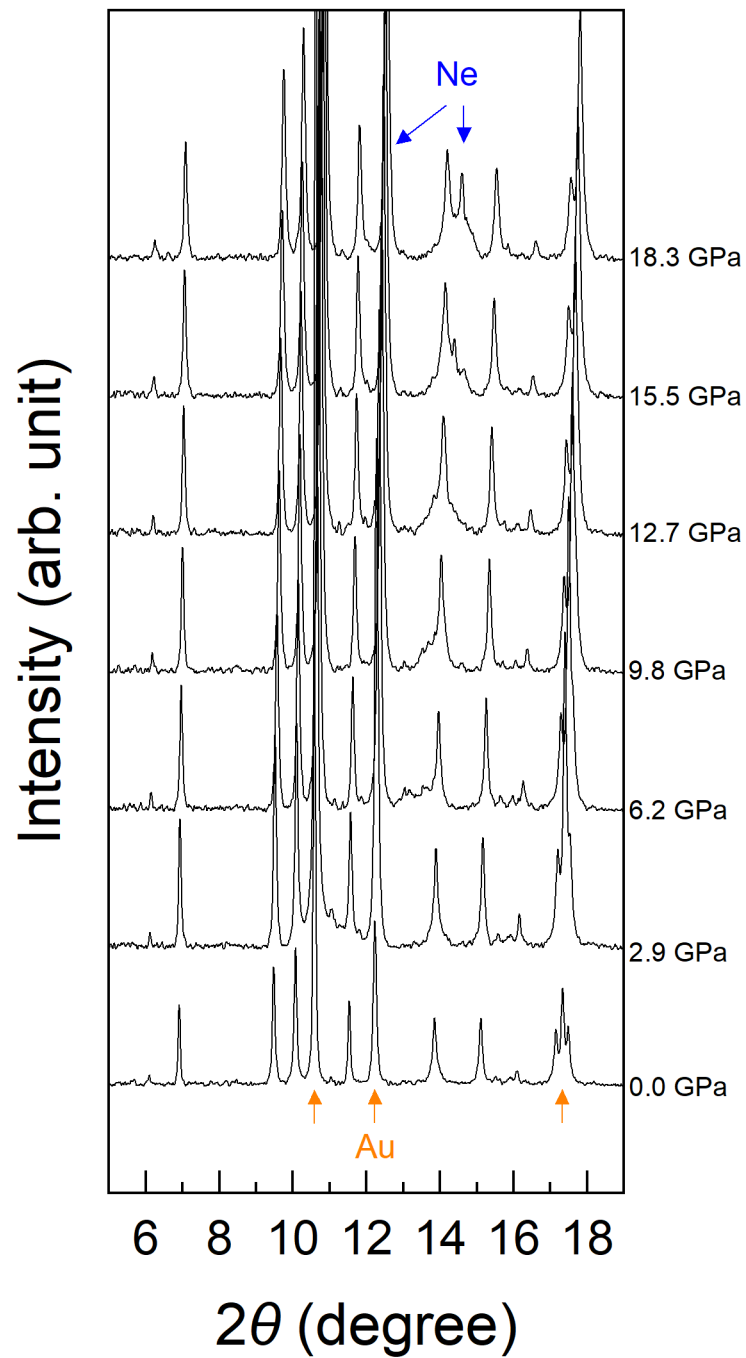


Figure S2. Stacked diffraction patterns from compression of synthetic

$(\text{Mg}_{0.46}\text{Fe}_{0.53}^{3+})(\text{Si}_{0.49}\text{Fe}_{0.51}^{3+})\text{O}_3$ from 1 bar to 18.3 GPa.

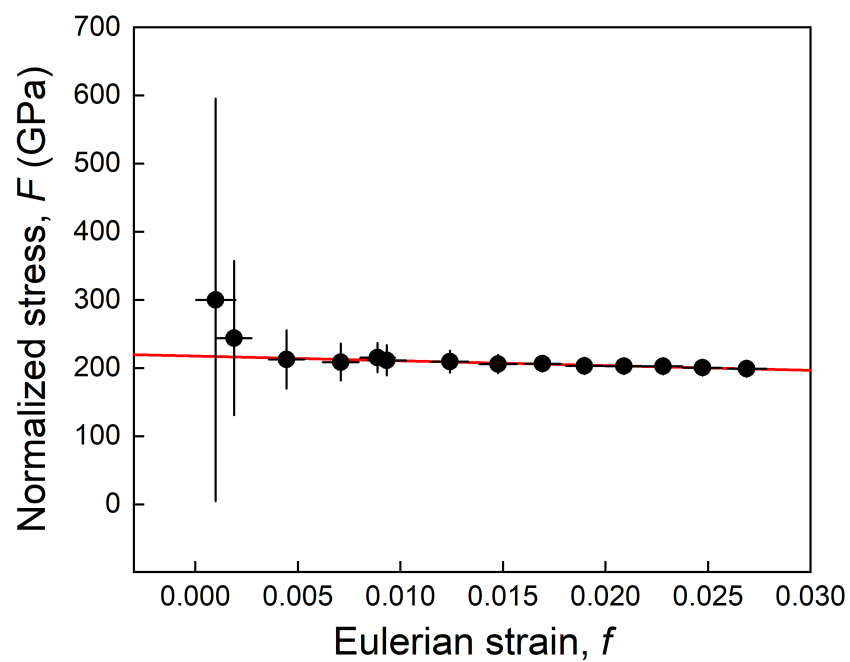


Figure S3. Normalized stress F vs. Eulerian strain f calculated from P - V data of Hem50-LN.

Table S1. Experimental and refinement details of Hem50-LN.

Space group	$R3c$
Lattice parameters (Å)	4.9496 (5), 4.9496 (5), 13.3138 (18)
Volume (Å ³)	282.47(7)
θ range for data collection	5.030-17.831
No. of reflections collected	143
No. of independent reflections	32
No. of parameters refined	9
Limiting indices	$-5 \leq h \leq 6$, $-5 \leq k \leq 5$, $-12 \leq l \leq 18$
R_{int}	0.1400
Final R_1 and wR_2 ($I > 2\sigma(I)$)	0.0711, 0.1630
Goodness of fit	1.423
$\Delta\rho_{\text{max}}$, $\Delta\rho_{\text{min}}$ (eÅ ⁻³)	1.190, -2.181

Table S2. Atomic coordinates and equivalent isotropic displacement parameters (\AA^2) for Hem50-LN. The following disorder model was used: (1) Fe1 and Mg have the same atomic coordination and atomic displacement parameters (ADPs), and the refined site of occupancy factor (SOF) of Mg for this site is ~ 0.5 ; (2) Fe2 and Si have the same atomic coordination and atomic displacement parameters (ADPs), and the refined site of occupancy factor (SOF) of Si for this site is ~ 0.5 ; (3) all Uiso values are positive.

	x	y	z	U (eq)	SOF
Mg, Fe1	0	0	0.6849(17)	0.002	0.5, 0.5
Si, Fe2	0	0	0.9712(6)	0.015	0.5, 0.5
O	0.96(2)	0.66(5)	0.9007(17)	0.002	1

Table S3. Observed volume and unit-cell parameters of Hem50-LN at 300 K. Au was used as the pressure standard.

P (GPa)	P uncertainty	a (Å)	a uncertainty	c (Å)	c uncertainty	V (Å ³)	V uncertainty
0.0	0.0	4.950	0.005	13.323	0.022	282.8	0.6
0.9	0.1	4.946	0.004	13.309	0.019	281.9	0.5
1.4	0.1	4.941	0.003	13.297	0.014	281.2	0.4
2.9	0.1	4.930	0.003	13.255	0.014	279.0	0.4
4.6	0.1	4.920	0.003	13.207	0.014	276.9	0.4
6.0	0.1	4.914	0.003	13.167	0.013	275.4	0.4
6.2	0.1	4.912	0.004	13.160	0.017	275.0	0.5
8.3	0.1	4.900	0.003	13.110	0.015	272.6	0.4
9.8	0.1	4.890	0.004	13.070	0.015	270.7	0.4
11.4	0.1	4.882	0.003	13.033	0.014	269.0	0.4
12.7	0.1	4.874	0.003	12.996	0.015	267.4	0.4
14.1	0.1	4.867	0.004	12.963	0.015	265.9	0.4
15.5	0.1	4.860	0.004	12.930	0.015	264.5	0.4
16.8	0.1	4.852	0.004	12.900	0.015	263.0	0.4
18.3	0.1	4.844	0.004	12.866	0.016	261.4	0.4

Table S4. Equation of state parameters of akimotoite, LN-type phase, and hematite.

Reference	V_0 (Å ³)	K_0 (GPa)	K'	Composition
This study	282.94(7)	211(3)	2.4(3)	(Mg _{0.46} Fe _{0.53} ³⁺)(Si _{0.49} Fe _{0.51} ³⁺)O ₃
This study	283.18(9)	198(1)	4(fixed)	(Mg _{0.46} Fe _{0.53} ³⁺)(Si _{0.49} Fe _{0.51} ³⁺)O ₃
This study	282.8(fixed)	204(1)	4(fixed)	(Mg _{0.46} Fe _{0.53} ³⁺)(Si _{0.49} Fe _{0.51} ³⁺)O ₃
Wang et al. (2004)	264.2(2)	210(fixed)	4.8(5)	MgSiO ₃
Zhou et al. (2014)	262.45(26)	207(3)	4.6(fixed)	MgSiO ₃
Hao et al. (2019)	261.83	211	4.37	MgSiO ₃
Siersch et al. (2021)	262.43(2)	205(1)	4.9(2)	MgSiO ₃
Bykova et al. (2016)	301.8(2)	219(7)	3.5(4)	Fe ₂ O ₃ (hematite)
Stixrude and Lithgow-Bertelloni (2022)	267.51	211(10)	5.2(10)	FeSiO ₃
Koemets et al. (2023)	266.35(8)	211(10)	4(fixed)	(Mg _{0.5} Fe _{0.5} ³⁺)(Si _{0.5} Al _{0.5})O ₃

References

- Bykova, E., Dubrovinsky, L., Dubrovinskaia, N., Bykov, M., McCammon, C., Ovsyannikov, S.V., Liermann, H.-P., Kuppenko, I., Chumakov, A.I., Rüffer, R., and others (2016) Structural complexity of simple Fe_2O_3 at high pressures and temperatures. *Nature Communications*, 7, ncomms10661.
- Hao, S., Wang, W., Qian, W., and Wu, Z. (2019) Elasticity of akimotoite under the mantle conditions: Implications for multiple discontinuities and seismic anisotropies at the depth of $\sim 600\text{--}750$ km in subduction zones. *Earth and Planetary Science Letters*, 528, 115830.
- Koemets, I., Wang, B., Koemets, E., Ishii, T., Liu, Z., McCammon, C., Chanyshiev, A., Katsura, T., Hanfland, M., Chumakov, A., and others (2023) Crystal chemistry and compressibility of $\text{Fe}_{0.5}\text{Mg}_{0.5}\text{Al}_{0.5}\text{Si}_{0.5}\text{O}_3$ and $\text{FeMg}_{0.5}\text{Si}_{0.5}\text{O}_3$ silicate perovskites at pressures up to 95 GPa. *Frontiers in Chemistry*, 11, 1258389.
- Siersch, N.C., Kurnosov, A., Criniti, G., Ishii, T., Ballaran, T.B., and Frost, D.J. (2021) The elastic properties and anisotropic behavior of MgSiO_3 akimotoite at transition zone pressures. *Physics of the Earth and Planetary Interiors*, 106786.
- Stixrude, L., and Lithgow-Bertelloni, C. (2022) Thermal expansivity, heat capacity and bulk modulus of the mantle. *Geophysical Journal International*, 228, 1119–1149.
- Wang, Y., Uchida, T., Zhang, J., Rivers, M.L., and Sutton, S.R. (2004) Thermal equation of state of akimotoite MgSiO_3 and effects of the akimotoite–garnet transformation on seismic structure near the 660 km discontinuity. *Physics of the Earth and Planetary Interiors*, 143–144, 57–80.
- Zhou, C., Gréaux, S., Nishiyama, N., Irifune, T., and Higo, Y. (2014) Sound velocities measurement on MgSiO_3 akimotoite at high pressures and high temperatures with simultaneous in situ X-ray diffraction and ultrasonic study. *Physics of the Earth and Planetary Interiors*, 228, 97–105.